Modulating the Water oxidation Catalytic activity of Iridium Complexes by Functionalizing the Cp*-Ancillary Ligand: Hints on the Nature of the Active Species

Giordano Gatto,[‡,⊥] *Alice De Palo,*[#,⊥] *Ana C. Carrasco,*[¥] *Ana M. Pizarro,*[¥] *Stefano Zacchini,*[§] *Guido Pampaloni,*[#] *Fabio Marchetti,*[*#] *and Alceo Macchioni*[*‡]

[‡]Department of Chemistry, Biology and Biotechnology and CIRCC, University of Perugia, Via Elce di Sotto 8, 06123 Perugia, Italy. [#]Dipartimento di Chimica e Chimica Industriale University of Pisa, Via G. Moruzzi 13, 56124 Pisa, Italy. [¥]IMDEA Nanociencia, Ciudad Universitaria de Cantoblanco, 28049 Madrid, Spain. [§]Dipartimento di Chimica Industriale "Toso Montanari", Università di Bologna, Viale Risorgimento 4, 40136 Bologna, Italy.

KEYWORDS: water oxidation, iridium complexes, active species, Nernst potential

ABSTRACT. The catalytic activity toward $NaIO_4$ driven water oxidation of a series of $[^{R}Cp^{*}IrCl(\mu\text{-}Cl)]_2$ dimeric precursors, containing tetramethylcyclopentadienyl ligands with a variable R substituent (H, **1**; Me, **2**; Et, **3**; ^{n}Pr, **4**; $CH_2CH_2NH_3^+$, **5**; Ph, **6**; 4-C_6H_4F, **7**; 4-C_6H_4OH, **8**; Bn, **9**) has been evaluated at 298 K and pH = 7 (by phosphate buffer). For each dimer, the effect of changing catalyst (1-10 μM) and $NaIO_4$ (5-40 mM) concentration has been studied. All

precursors exhibit a high activity with TOF values ranging from 101 min^{-1} to 393 min^{-1} and TON values being always those expected assuming a 100% yield. The catalytic activity was strongly affected by the nature of the R substituent. Highest TOF values were observed when R was electron-donating and small. The results of multiple injection consecutive experiments suggest that a fragment of the initial C_5Me_4R, still bearing the R-substituent, remains attached at iridium in the active species, despite the oxidative *in situ* degradation of the same ligand. The decrease of TOF in the second and third catalytic runs was completely ascribed to a drop of the redox potential caused by the conversion of IO_4^- into IO_3^-, according to the Nernst equation. This hypothesis was verified by performing catalytic experiments in which the initial redox potential (ΔE) was deliberately varied by using water solutions of IO_4^-/IO_3^- mixtures at different relative concentrations. Consistently, TOF *versus* ΔE plots show that, for a given catalyst, the same TOF is obtained at a certain redox potential, irrespectively of the initial reaction conditions used.

1. INTRODUCTION

The development of efficient catalysts for water oxidation (WOCs) remains the main obstacle to the assembly of a working device for the production of fuels from renewable sources.[1–6] Considerable progress has been achieved, over the last few years, with material-based,[7–11] heterogenized,[12–18] and molecular WOCs.[19–26] Among the latter, organoiridium complexes have been successfully exploited as precursors of WOCs.[27,28] Most of them can be formulated as $[Cp^*IrL_1L_2X]^n$ where L_1 and L_2 might be either two monodentate or one bidentate ligand(s), whereas X is H_2O or a labile ligand easily exchangeable with a water molecule. Despite many studies have been performed to understand how the nature of L_1 and L_2 affects WO performances, to the best of our knowledge very little (or no) attention has been dedicated to

explore the possible effect of functionalizing the Cp* ancillary ligand.[29] This is probably due to the difficulty of synthesizing Cp*-substituted precursors and also to the belief that Cp* is easily lost under the strongly oxidative conditions used in WO catalysis. As a matter of fact, many studies, initially carried out by NMR spectroscopy, indicated that the Ir–C bond of the quaternary Cp* ligand is the weak point of $[Cp^*IrL_1L_2X]^n$ WOC,[30] which can be easily oxidized opening reaction pathways leading to the oxidative transformation of Cp*, causing the degradation of the latter and formation of small molecules such as CH_3COOH, HCOOH, CH_2COOH, and CO_2.[31–33] At the same time, organometallic species having an oxidatively degraded Cp* still bonded at iridium, but with reduced hapticity, have been observed, in some cases.[33] Interestingly, the rate of CH_3COOH and HCOOH formation, two important degradation products of Cp*, was found to be substantially higher than that of O_2 evolution, indicating that the oxidative degradation occurs in the preliminary stage of the catalysis, likely during the induction time, and leads to the formation of the active species carrying on most O_2 evolution process.[34] Nevertheless, to the best of our knowledge, no investigation demonstrated that Cp* is completely degraded during such a preliminary stage. On the contrary, the few attempts aimed at quantifying the small organic oxidized fragments indicated that two/three carbon atoms of Cp* are apparently missing and many hypotheses on the nature of WO active species have been proposed according to which a part of the Cp* is still coordinated to the iridium.[35,36] For instance, Batista suggested a dimeric complex bearing a methyl-acetone-acetonate moiety, bonded at each iridium atom and derived from Cp* oxidative degradation.[37]

In order to shed some light on how the functionalization of Cp* affects WO catalyzed by $[Cp^*IrL_1L_2X]^n$ catalysts, we decided to synthesize a series of Ir-dimers with R-functionalized Cp*, i.e. $([(\eta^5\text{-}C_5Me_4R)IrCl(\mu\text{-}Cl)]_2$: R = H, **1**; R = Me, **2**; R = Et, **3**; R = ^{n}Pr, **4**; R =

$CH_2CH_2NH_3^+$, **5**; R = Ph, **6**; R = 4-C_6H_4F, **7**; R = 4-C_6H_4OH, **8**; R = Bn, **9**; Figure 1) and test them as WO catalytic precursors. WO catalytic experiments were carried out using $NaIO_4$ as sacrificial oxidant at pH = 7 (by phosphate buffer) and at 298 K. For each dimer, seven experiments were carried out, changing catalyst and $NaIO_4$ concentration, according to a standardized methodology recently applied by us to benchmarking a rather large number of well-known iridium WOCs.[38]

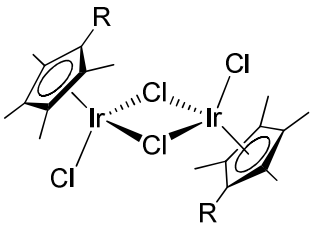

Figure 1: Sketch of the investigated Ir-dimers.

It was found that the WO catalytic activity is strongly affected by the nature of R with best performances obtained when electron donating and small R-substituents are used.

2. RESULTS AND DISCUSSION

The neutral di-iridium complexes, including the novel **1**, **3-4**, **7-8**, were obtained in moderate yields using a typical procedure consisting in the reaction of commercial iridium(III) chloride hydrate with the appropriate substituted cyclopentadiene precursor in refluxing methanol (Scheme 1).[39,40] The ammonium chloride salt **5** was obtained following a literature procedure whereby the cyclopentadiene $C_5HMe_4CH_2CH_2NH_2{\cdot}HCl$ and $[IrCl(COD)]_2$ were allowed to react in the presence of HCl. The cyclopentadiene C_5HMe_4(4-C_6H_4F) is unprecedented, while C_5HMe_4(4-C_6H_4OH) was synthesized by a modified literature method (see Experimental for

details).[41] Both these pro-ligands were isolated as almost exclusively single isomeric forms.[39] In order to prepare **8**, the hydroxyl group of $C_5HMe_4(4\text{-}C_6H_4OH)$ was preliminarily protected, then the reaction of $C_5HMe_4(4\text{-}C_6H_4OCMe_2OMe)$ with $IrCl_3 \cdot nH_2O$, followed by silica chromatography, directly afforded **8**. The new mononuclear **10** and **11** were obtained from **1** and **4**, respectively, by reaction with picolinic acid (pic) and finally isolated in 40% (**10**) and 76% (**11**) yields. All the iridium complexes, except **5** and **8**, are well soluble in chlorinated solvents and exhibit very low solubilities in water and hydrocarbons; instead, **5** and **8** are soluble in methanol and dimethylsulfoxide, and **5** also in water. The new complexes were characterized by elemental analysis, IR and NMR spectroscopy, and their identity was confirmed by mass spectrometry. The ^1H and ^{13}C NMR patterns related to the $\{C_5Me_4\}$ unit are consistent with what previously reported for similar species.[39] The CH moiety belonging to the five-membered C_5HMe_4 ring in **1** gives raise to resonances at 5.30 ppm (^1H) and 68.1 ppm (^{13}C). The hydroxyl group in **8** manifests itself with an absorption falling at 3305 cm^{-1} in the IR spectrum (solid state). The ^{19}F NMR resonance due to the fluorine atom undergoes minor shift on going from $C_5HMe_4(4\text{-}C_6H_4F)$ (−117.6 ppm) to **7** (−112.7 ppm).

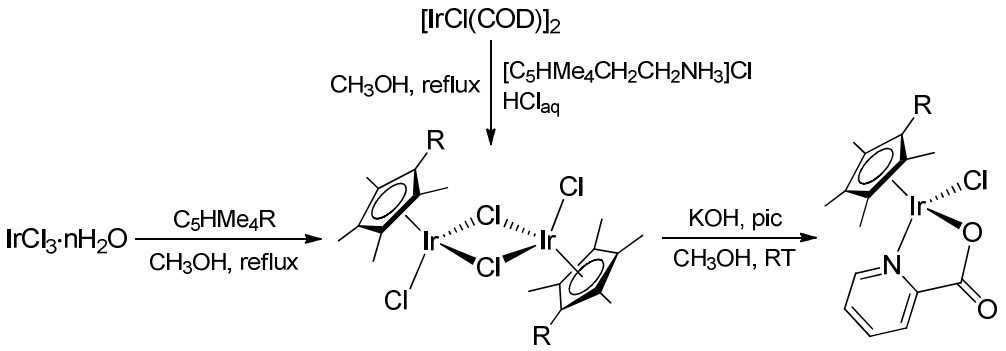

	R	
1	H	**10**
2	Me	
3	Et	

4	Pr	**11**
5	$CH_2CH_2NH_2{\cdot}HCl$	
6	Ph	
7	$4\text{-}C_6H_4F$	
8	$4\text{-}C_6H_4OH$ [a]	
9	Bn	

Scheme 1: Synthesis of di- and mono-iridium complexes. [a]From $C_5HMe_4(4\text{-}C_6H_4OCMe_2OMe)$.

The molecular structures of **7** and **11** were ascertained by X-ray diffraction studies. The molecular structure of **7** (Figure 2) is closely related to that previously reported for complex **6**, the latter differing from the former in that the phenyl rings do not contain a F-substituent. The $Ir(\mu\text{-}Cl)_2Ir$ core is perfectly planar (mean deviation from the least squares plane 0.0079 Å) and the two $^{F\text{-}Ph}Cp^*$ ligands adopt a *pseudo-trans* conformation.

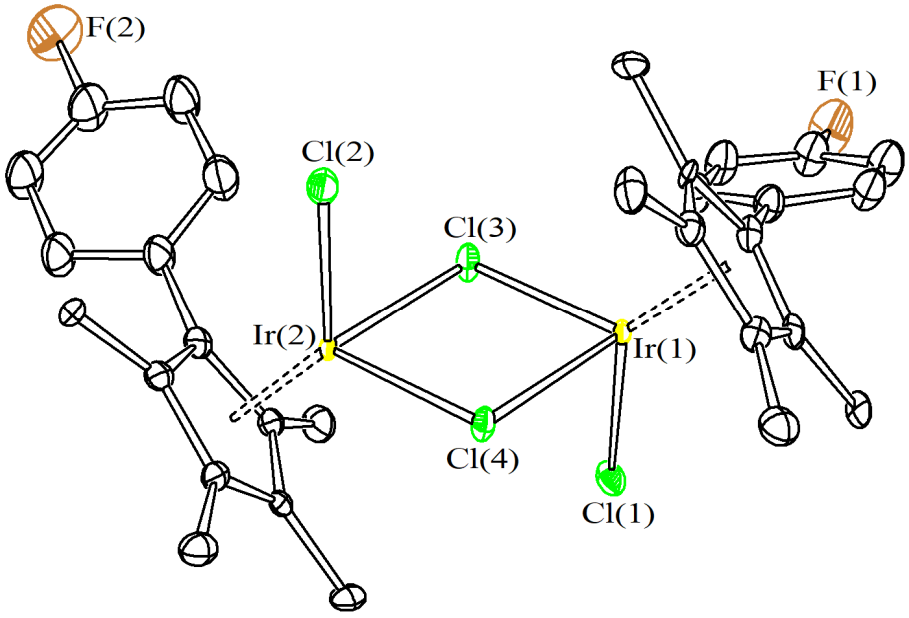

Figure 2. Molecular structure of $[^{F\text{-}Ph}Cp^*IrCl(\mu\text{-}Cl)]_2$, **7**. Displacement ellipsoids are at the 50% probability level. H-atoms have been omitted for clarity. Selected bond lengths (Å) and angles (°): Ir(1)–Cl(1) 2.382(3), Ir(1)–Cl(3) 2.450(3), Ir(1)–Cl(4) 2.457(3), Ir(1). $^{F\text{-}Ph}Cp^*$ 2.115(14)–

2.157(13), Ir(2)−Cl(2) 2.386(3), Ir(2)−Cl(3) 2.442(3), Ir(2)−Cl(4) 2.454(3), Ir(2)–$^{F\text{-}Ph}$Cp*2.115(14)– 2.161(13), Cl(3)–Ir(1)–Cl(4) 88.56(13), Cl(3)–Ir(2)–Cl(4) 88.13(13), Ir(1)–Cl(3)–Ir(2) 99.23(13), Ir(1)–Cl(4)–Ir(2) 98.71(12).

The geometry and bonding parameters of **11** (Figure 3) are analogous to those reported for related piano-stool complexes where Ir^{III} is bonded to a C_5Me_5[42–44] or a C_5Me_4Ph[40] ring, one chelating picolinato ligand and one terminal chloride. In particular, the replacement of one methyl substituent with a propyl one (compound **11**) on the cyclopentadienyl moiety does not determine any significant change in the distances between the iridium center and the atoms bound to it.

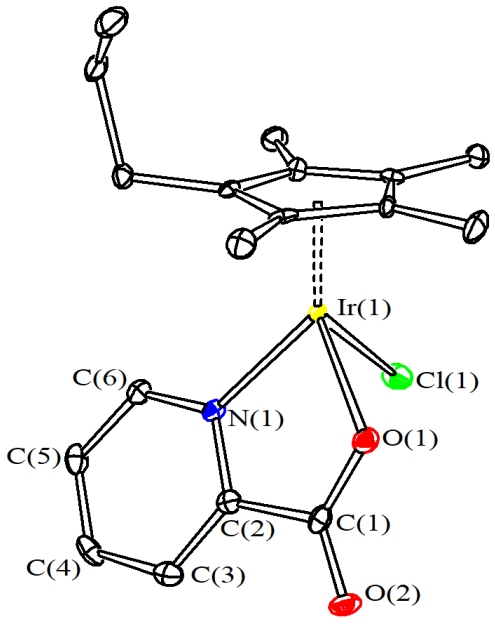

Figure 3. Molecular structure of [^{Pr}Cp*IrCl(pic)], **11**. Displacement ellipsoids are at the 50% probability level. H-atoms have been omitted for clarity. Selected bond lengths (Å) and angles (°): Ir(1)−Cl(1) 2.4014(11), Ir(1)−N(1) 2.083(4), Ir(1)−O(1) 2.104(3), Ir(1)–^{Pr}Cp* 2.130(4)-2.170(4), C(1)−O(1) 1.284(5), C(1)−O(2) 1.227(5), C(1)−C(2) 1.509(6), O(1)−Ir(1)−N(1)

77.43(13), Ir(1)−N(1)−C(2) 115.1(3), N(1)−C(2)−C(1) 115.0(3), C(2)−C(1)−O(1) 114.6(4), C(1)−O(1)−Ir(1) 116.9(3), C(2)−C(1)−O(2) 119.6(4), O(2)−C(1)−O(1)125.8(4).

All complexes shown in Scheme 1 exhibit high activity with TOF_{max} values included between 393 min^{-1} and 101 min^{-1}, depending on the nature and concentration of the complex, and on the concentration of $NaIO_4$ (Tables S1-S4). For each dimer, the orders in iridium and $NaIO_4$ were determined by varying the catalyst concentration (1, 2.5, 5, and 10 μM) at [$NaIO_4$] = 20 mM and the $NaIO_4$ concentration (5, 10, 20, 40 mM) at [Ir] = 5 μM, respectively. The orders in iridium and $NaIO_4$ are close to 1 and 0.5, respectively, for all catalysts (Supporting Information).

Six graphs are reported in the Supporting Information for each catalyst, showing: i) TON versus t at different catalyst concentrations; ii) TOF versus time at different catalyst concentrations; iii) TOF versus X at different catalyst concentrations; iv) TON versus t at different $NaIO_4$ concentrations; v) TOF versus time at different $NaIO_4$ concentrations; and vi) TOF versus X at different $NaIO_4$ concentrations. An example of such graphs is reported in Figure 4 for the dimer **1**. Looking at the plots of Figure 4, and the analogous ones reported in the Supporting Information, it is clear that dimers **1**–**9** act as extremely efficient WOCs. From TON versus t and TOF versus t trends, it is evident that all moles of O_2 expected, based on the amount of $NaIO_4$ used, are formed at every catalyst and $NaIO_4$ concentrations. TOF versus X plots are instead useful to graphically evaluate the order in catalyst according to reaction progress kinetic analysis (RPKA) proposed by Blackmond.[45,46] For instance, because the TOF versus X plots at different catalyst concentration values show a substantial overlap (Figure 4 and Supporting Information), it can be immediately concluded that the reaction order in catalyst is 1. TOF versus X plots can also provide important information about the tendency of catalysts to activate.

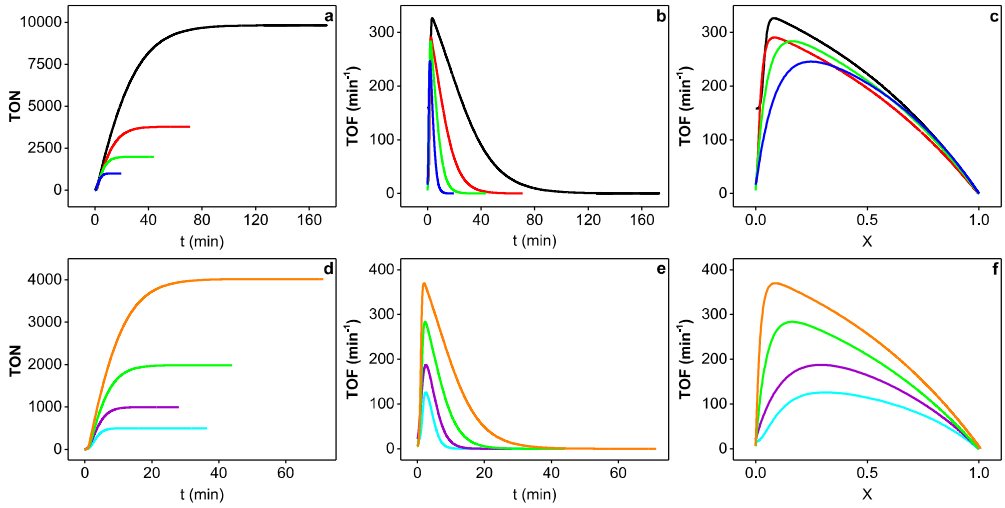

Figure 4: Kinetic trends for catalyst **1** (water solution at pH 7 by phosphate buffer 0.2 M, 25°C) at different iridium (a, b, c: black, 1 μM; red, 2.5 μM; green, 5 μM; blue, 10 μM) and $NaIO_4$ (d, e, f: orange, 40 mM; green, 20 mM; violet, 10 mM; cyan, 5 mM) concentrations.

As stated above, the reaction yield is always close to 100% with $TON_{max} \approx 10000$. The dimeric complexes show the following relative scale of average TOF values (calculated on all the individual TOF values of the seven experiments carried out at different [Ir] and [$NaIO_4$]): **2** (Me, 299 min^{-1}) ≥ **3** (Et, 285 min^{-1}) ≥ **1** (H, 260 min^{-1}) ≥ **5** ($CH_2CH_2NH_2$·HCl, 244 min^{-1}) ≈ **4** (^{n}Pr, 239 min^{-1}) ≥ **9** (Bn, 216 min^{-1}) ≥ **8** (4-C_6H_4OH, 193 min^{-1}) ≈ **6** (Ph, 192 min^{-1}) ≥ **7** (4-C_6H_4F, 177 min^{-1}). By comparing the blue series reported in Figure 5, in which the steric hindrance of R is varied, whereas its electronic contribution is approximately constant, it appears evident that the catalytic activity of dimers is significantly decreased when the steric hindrance of R increases. As a matter of fact, averaged TOF decreases from 299 min^{-1} for **2** (Me) down to 216 min^{-1} for **9** (Bn). It is also evident that less electron donating R substituents have a detrimental effect on the activity of dimers. Indeed, aryl-substituted Cp* dimers (green in Figure 5) exhibit considerably

lower averaged TOF values than alkyl substituted ones (blue in Figure 5). Interestingly, dimer **5**, having a dangling substituent ($CH_2CH_2NH_3^+$), behaves exactly as the isosteric complex **4** (^{n}Pr, red bar in Figure 5); since it has been shown in complexes analogous to **5** that the amine function may coordinate the metal center leading to mononuclear derivatives, the experimental evidence suggests that the ammonium group in **5** is not deprotonated under the catalytic conditions. Finally, the electronic factor appears to be predominant over the steric factor in **1** (H), which shows an average TOF (yellow bar in Figure 5) significantly lower than **2** (Me) and even **3** (Et).

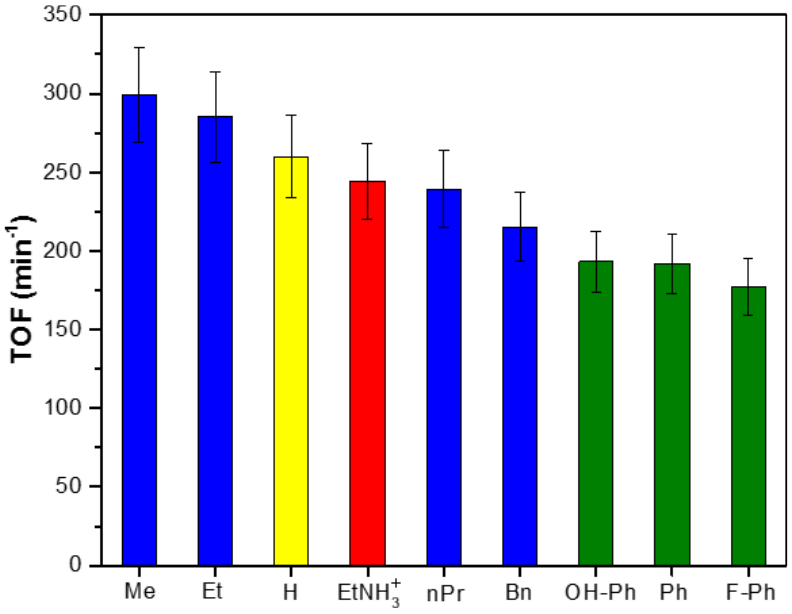

Figure 5. Average TOF values for $NaIO_4$ driven WO catalyzed by dimeric complexes **1**-**9** (water solution at pH 7 by phosphate buffer 0.2 M, 25°C, error bar = 10%).

Based on the results of previous studies, indicating, at least, a partial degradation of the Cp* ligand,[33] the observed catalytic trends can be interpreted in two different ways: i) a fragment of C_5Me_4R, still bearing the R-substituent, remains attached at iridium in the active species (hypothesis 1); ii) the active species is the same independently of R, nevertheless, the latter

affects the achievement rate and/or the amount of the active species (hypothesis 2). If hypothesis 1 were correct, it would be reasonable to conclude that an oxidative step of the water oxidation catalytic cycle is the turnover limiting step, since catalysis is favored by more electron donating substituents, and the achievement of the active species is an associative process, because it is disfavored by bulky substituents. In case hypothesis 2 were correct, it could be presumed that more electron-donating C_5Me_4R groups might undergo faster oxidative transformation, since they are more strongly coordinated at iridium and, consequently, more activated toward oxygen attack, whereas bulkier substituents ask for more oxidative equivalents to be degraded, which are subtracted to catalysis, thus reducing the efficiency. In order to discriminate between the two hypotheses, multiple injections consecutive catalytic experiments have been performed for the fastest (**2**) and slowest (**7**) catalysts (Table S5). The rationale underlying such an experiment is that if the active species is the same for all complexes (hypothesis 2), the difference in the TOF of the two catalysts should become smaller and smaller or even vanish in runs successive to the first. The results are reported in Figure 6.

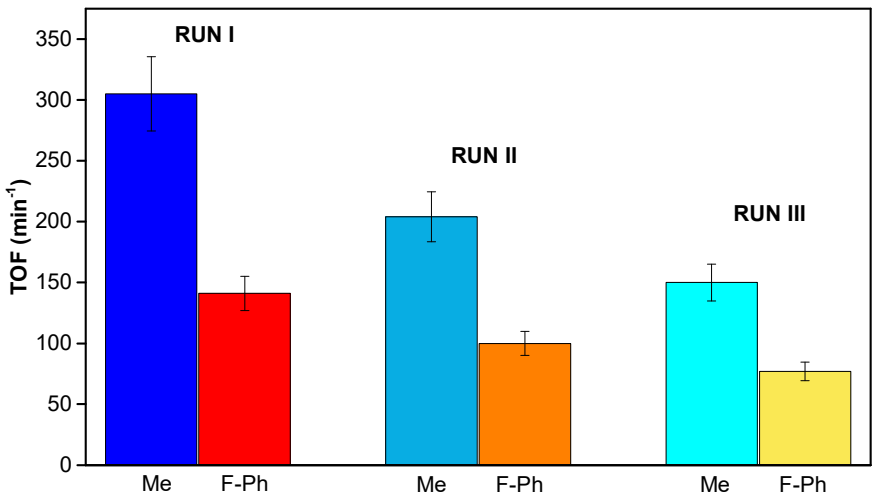

Figure 6. TOF values for $NaIO_4$ driven WO catalyzed by dimeric complexes **2** and **7** (water solution at pH 7 by phosphate buffer 0.2 M, 25°C, error bar = 10%) in triple run experiments.

Both **2** and **7** exhibit significant decrease of TOF passing from the first [**2**, 305± 31 min^{-1}; **7**_Ph_F, 141± 14 min^{-1}] to the second [**2**, 204± 20 min^{-1}; **7**, 100± 10 min^{-1}] and third [**2**_Me, 150± 15 min^{-1}; **7**_Ph_F, 79± 8 min^{-1}] run. Nevertheless, it is clear that their activity is not the same in each run: this finding supports hypothesis 1. The observed reduced TOF in the second and third runs might be due to a decrease of the redox potential due to the presence of IO_3^-, according to the Nernst equation ($E = E^0 – RT/nFln([IO_4^-]/[IO_3^-])$. Because TOF should be a function of ΔE (where $\Delta E = E – E^0 = –RT/nFln([IO_4^-]/[IO_3^-])$,[47] this can be verified by plotting the measured TOF at any time as a function of ΔE for all three consecutive runs (Figure 7).

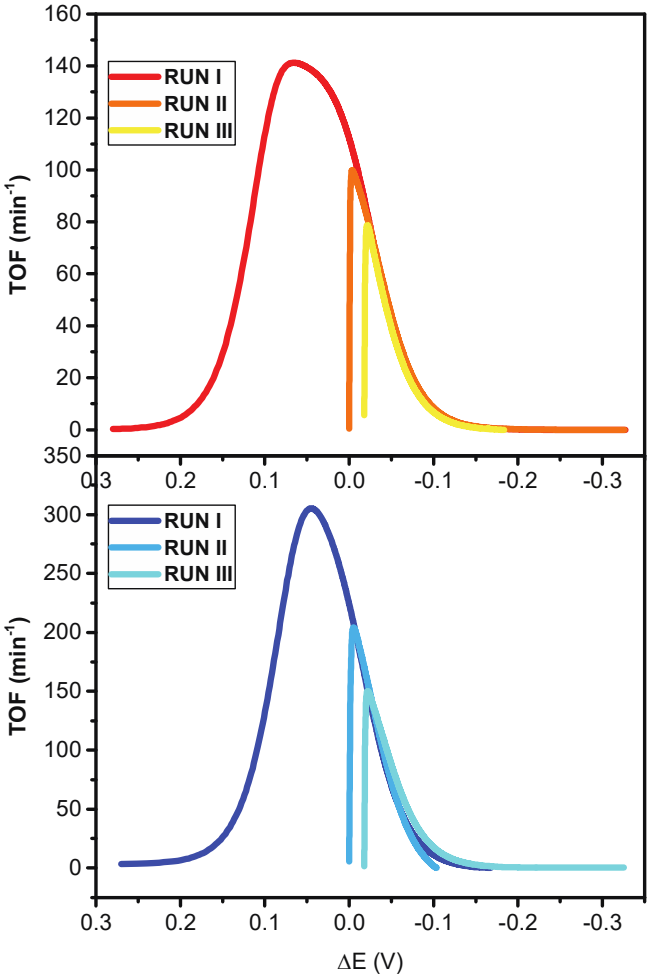

Figure 7. TOF *versus* ΔE for $NaIO_4$ driven WO catalyzed by the dimeric complex **2** (down) and **7** (top) (water solution at pH 7 by phosphate buffer 0.2 M, 25°C) in a triple run experiment showing that at the same redox potential TOF values are the same in all three experiments.

Before discussing the trends, it is important to outline that the initial decrease of ΔE from ca. 0.3 V down to the value corresponding to TOF_{MAX}, ca. 0.15 V, occurs very rapidly (t_{MAX} = 1.6 min and 2.5 min for **2** and **7**, respectively; X_{MAX} = 0.13 and 0.08 for **2** and **7**, respectively). Whereas the second part of the trends in Figure 7, from TOF_{MAX} on, is responsible for most of the reaction time. For example, ΔE = –0.1 V is reached at t = 16.9 min and 30.3 min, for **2** and **7**, respectively

(X = 0.98 for both precursors). It is reasonable to believe that during the initial growth of TOF a sort of activation is occurring leading to the transformation of the precursors into the active species. Interestingly, after that period, the three trends are perfectly coherent and the same TOF are observed for the three catalytic runs at the same potential value. This is a strong indication that the active species is the same during all the catalytic runs. The same coherent trends are observed for **7**, clearly with different TOF values with respect to those of **2**. This means that also in this case the same active species is present in all three catalytic runs that, nevertheless, has to be different from that derived from **2**. It seems reasonable to deduce that a fragment of $^{R}Cp^{*}$ still containing R has to be present in the active species, consistently with hypothesis 1. Another battery of experiments has been performed to enforce hypothesis 1. Catalytic runs were carried out for **2** at a definite initial redox potential injecting fresh catalyst into a water solution of a mixture of IO_4^-/IO_3^-. In such experiments the following concentrations were used: $[IO_4^-]$ = 20 mM and $[IO_3^-]$ = 0 mM, 1 mM, 5 mM, 10 mM, 20 mM, and 40 mM. Furthermore, for each starting situation the second run (and in one case a third run) was also recorded. All catalytic experiments (first and second runs) are perfectly coherent in that exactly the same TOF is always observed at the same redox potential (Figure 8). Consistently, the same trends are observed for the successive runs and the ones with the fresh catalyst, when the initial IO_4^-/IO_3^- ratio is the same.[48] This is, in our opinion, an unambiguous demonstration that the active species must be always the same and should, consequently, contain a fragment of the initial $^{R}Cp^{*}$ still bearing R.

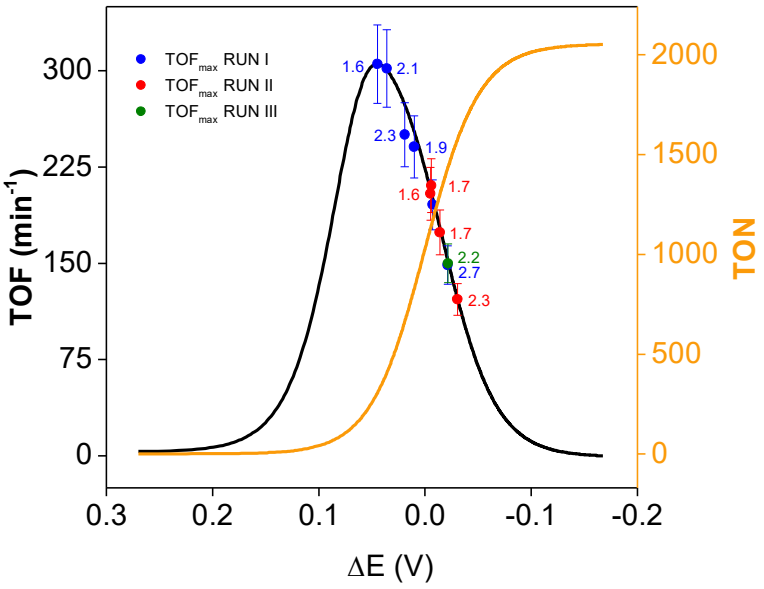

Figure 8. TOF (black) and TON (orange) *versus* ΔE trend for $NaIO_4$ (20 mM) driven WO catalyzed by the dimeric complex **2** (5 μM, water solution at pH 7 by phosphate buffer 0.2 M, 25°C). Blue (RUN I), red (RUN II) and green (RUN III) points represent the TOF_{MAX}/ΔE pair of values of independent catalytic runs carried out in the presence of variable amount of $NaIO_3$. Numbers near the error bar indicate the time (expressed in minutes) at which TOF_{max} is reached for each individual catalytic run.

3. CONCLUSIONS

The effect of functionalizing the Cp* on the catalytic activity of organometallic Ir WOCs has been explored. At this aim, a series of complexes of formula $[(\eta^5\text{-}C_5Me_4R)IrCl(\mu\text{-}Cl)]_2$ were synthesized, fully characterized, and tested in WO driven by $NaIO_4$. All complexes exhibited remarkable performances and, more importantly, their investigation provided clear evidence for the active species containing an R-substituted fragment, derived from the oxidative degradation of the C_5Me_4R ligand. As a matter of fact, the nature of R significantly affected catalytic activity,

which increased on decreasing the steric hindrance and enhancing electron-donating tendency of the R group. Furthermore, multiple injection catalytic experiments evidenced that the R-effect on catalytic performance persists in the second and third runs, ruling out the hypothesis that an identical active species is generated from all the different precatalysts. TOF *versus* ΔE (redox potential) plots shed some additional light on the nature and generation of the active species. They indicate that, after a short activation period, during which the transformation of the precursors occurs, individual active species for each dimer form, through an oxidative and associative turnover limiting step, and remain the same also after multiple additions of sacrificial oxidant. It can be therefore speculated that such active species are small iridium clusters bearing R-functionalized likely O,O-bidentate ligands.

4. EXPERIMENTAL SECTION

Synthesis and characterization of compounds

General details. Organic reactants were commercial products (TCI Europe or Merck) of the highest purity available. Solvents were purchased from Merck and, when required, distilled before use over appropriate drying agents. $IrCl_3 \cdot nH_2O$ was purchased from Merck, and $IrCl(COD)]_2$ from Alfa Aesar. The cyclopentadienes $C_5HMe_4(CH_2CH_2NH_2 \cdot HCl)$ and $C_5HMe_4(Bn)$ and the complexes **2**,[49] **5**, **6**[39] and **9**[39] were prepared according to the respective literature procedures. Infrared spectra of solid samples were recorded on a Perkin Elmer Spectrum One FT-IR spectrometer, equipped with a UATR sampling accessory (4000-400 cm^{-1} range). UV-Vis spectra were recorded on an Ultraspec 2100 Pro spectrophotometer. IR and UV-Vis spectra were processed with Spectragryph software.[50] NMR spectra were recorded at 298 K on a Bruker Avance II DRX400 instrument equipped with a BBFO broadband probe. Chemical

shifts (expressed in parts per million) are referenced to the residual solvent peaks[51] (^{1}H, ^{13}C) or to external standard (^{19}F, $CFCl_3$). NMR spectra were assigned with the assistance of ^{1}H-^{13}C (*gs*-HSQC and *gs*-HMBC) correlation experiments.[52] NMR signals due to a second isomeric form are italicized. Carbon, hydrogen and nitrogen analyses were performed on a Vario MICRO cube instrument (Elementar). Mass spectrometry measurements in positive ion scan mode were performed with an API 4000 instrument (SCIEX), equipped with an electrospray source.

$C_5HMe_4(4\text{-}C_6H_4F)$. A solution of 2,3,4,5-tetramethyl-2-cyclopentenone (0.950 g, 1.09 mL, 6.87 mmol) in anhydrous THF (10 mL) was cooled down to -78°C with a dry ice-acetone bath, then a solution of 4-fluorophenylmagnesium bromide (14.5 mL, 14.5 mmol) in THF was added dropwise. The mixture was stirred for 1 hour at -78°C, and then allowed to warm to room temperature and stirred for additional 20 hours. The resulting reaction mixture was cooled to 0 °C and quenched with HCl (20 mL of a 1 M aqueous solution, 20 mmol). The obtained yellow solution was warmed to room temperature and stirred for 1 hour. The organic phase was washed with water (30 mL x 3) and dried over $MgSO_4$. The crude product was purified by alumina column chromatography, using pentane as eluent. A yellow solid was obtained upon solvent removal under vacuum. Yield: 0.577 g, 40%. IR (solid): $\tilde{\upsilon}/cm^{-1}$ = 3072w, 2919w, 1748w, 1484w-m, 1448m, 1379m, 1085m, 1020vs, 797m-s, 736w-m, 689w.^{1}H NMR ($CDCl_3$): δ/ppm = 7.20, 7.07 (m, 4 H, C_6H_4), 3.17 (m, 1 H, MeC*H*), 2.02 (d, $^{4}J_{HH}$= 1.5 Hz, 3 H, C*Me*), 1.95, 1.89 (s, 6 H, C*Me*), 0.96 (d, 3 H, $^{3}J_{HH}$ = 7.34 Hz, MeC*H*). ^{13}C NMR (400 MHz, $CDCl_3$): δ/ppm = 161.0 (d, $^{1}J_{CF}$ = 244 Hz, CF),141.7, 140.6, 137.1, 135.0 (*C*Me), 133.3 (*C*-C_5Me_4), 129.4 (d, $^{3}J_{CF}$ = 7.4Hz, C_6H_4), 115.0 (d, $^{2}J_{CF}$ = 20.8 Hz, C_6H_4), 50.3 (*C*HMe), 14.5, 12.6, 11.9, 11.1 (C*Me*). ^{19}F NMR (400 MHz, $CDCl_3$): δ/ppm = *–115.7*, *–116.7*, –117.6. Isomer ratio ca. 1 : 1.5 : 32. Signals due to secondary isomeric forms are italicized. ESI-MS(+) *m/z* = 217.1 $[M+H]^+$.

$C_5HMe_4(4\text{-}C_6H_4OH)$.[41] The title compound was obtained by using a modified literature procedure.[41] 2-Methoxypropene (3.0 mL, 0.031 mol) was added to 4-C_6H_4(Br)(OH) (2.63 g, 0.015 mol), then a drop of $POCl_3$ was added to the mixture, which was stirred at room temperature for 1 hour under protection from the light. Then few drops of NEt_3 were added, and the volatile materials were removed under reduced pressure. The resulting colourless oil, corresponding to 1,4-C_6H_4(Br)($OCMe_2OMe$), was dissolved in Et_2O (20 mL) under N_2atmosphere. The solution was cooled to ca. −70 °C, and a 2.5 M solution of butyllithium in hexanes (6.0 mL, 0.015 mol) was added dropwise. The solution was stirred for 90 min during which time it was allowed to warm to room temperature. The final mixture was cooled to ca. −70°C and treated dropwise with 2,3,4,5-tetramethyl-2-cyclopentenone (2.3 mL, 0.015 mol) under nitrogen atmosphere. The resulting yellow solution was stirred overnight, then it was quenched with H_2O (2 mL). A yellow mixture was obtained which was stirred for additional 10 minutes. The liquid was separated, and the residue was washed with Et_2O (2 x 20 mL) in order to extract more organic substrate. The collected organic phases were eliminated of the volatiles under vacuum, thus affording a dark brown oil, which was dried over P_2O_5 overnight. Yield: 2.70 g, 83% respect to 4-C_6H_4(Br)(OH). ^{1}H NMR (400 MHz, $CDCl_3$): δ/ppm = 7.11, 6.89 (d, 2 H, $^3J_{HH}$ = 8.31 Hz, C_6H_4), 4.93 (br, 1 H, OH), 3.13 (m, 1 H, MeC*H*), 2.00, 1.93, 1.86 (s, 9 H, C*Me*), 0.94 (d, 3 H, $^3J_{HH}$ = 7.83 Hz, Me*C*H).

$C_5HMe_4(4\text{-}C_6H_4OCMe_2OMe)$.[41] C_5HMe_4(4-C_6H_4OH) (2.05 g, 9.57 mmol) was treated with 2-methoxypropene (1.8 mL, 19 mol), then a drop of $POCl_3$ was added to the mixture. The resulting mixture was stirred at room temperature for 1 hour, and then quenched with five drops of NEt_3. Removal of the volatiles under reduced pressure afforded an orange-brown oil, which was purified by filtration through an alumina column using Et_2O as eluent. Yield: 2.32 g, 85%. ^{1}H

NMR (400 MHz, $CDCl_3$): δ/ppm = 7.17, 7.15 (d, 2 H, C_6H_4); 3.47 (s, 3 H, OMe); 3.15 (m, 1 H, MeC*H*); 2.03, 1.94, 1.88 (s, 9 H, C*Me*); 1.52 (s, 6 H, C*Me*$_2$); 0.97 (d, 3 H, $^3J_{HH}$ = 7.34 Hz, *Me*CH).

[^{H}Cp*IrCl(μ-Cl)]$_2$ (1). A solution of tetramethylcyclopentadiene (0.38 mL, 2.1 mmol) and $IrCl_3 \cdot nH_2O$ (54.6% of Ir, 0.500 g, 1.42 mmol) in degassed MeOH (20 mL) was heated at reflux for 48 hours. Then the resulting mixture was allowed to cool to room temperature, concentrated under reduced pressure and stored at –30 °C for 24 hours. An orange precipitate was recovered, washed with cold methanol and diethyl ether and dried under vacuum. Yield: 0.128g, 23%. Anal. calcd. for $C_{18}H_{26}Cl_4Ir_2$: C, 28.13; H, 3.41. Found: C, 28.21; H, 3.50. IR (solid): ῡ/cm^{-1} = 3072w, 2919w, 1748w, 1484w-m, 1448m, 1379m, 1085m, 1020vs, 797m-s, 736w-m, 689w.^{1}H NMR (400 MHz, $CDCl_3$): δ/ppm = 5.30 (s, 1 H, C_5Me_4H), 1.70, 1.65 (s, 12 H, Me). ^{13}C NMR (400 MHz, $CDCl_3$): δ/ppm = 91.8, 86.3 (*C*Me), 68.1 (*C*H), 11.0, 9.3 (C*Me*). ESI-MS(+) *m/z* = 733.0 $[M–Cl]^+$.

[^{Et}Cp*IrCl(μ-Cl)]$_2$ (3). A solution of tetramethyl(ethyl)cyclopentadiene (0.31 mL, 1.8 mmol) and $IrCl_3 \cdot nH_2O$ (54.6% of Ir, 0.400 g, 1.17 mmol) in degassed MeOH (20 mL) was heated at reflux for 48 hours. The resulting mixture was allowed to cool to room temperature, filtered to eliminate some dark solid, and concentrated under reduced pressure. The crude product was purified by washing with diethyl ether (2 x 20 mL) and subsequent crystallization from a double layer CH_2Cl_2/hexane at -30 ºC, affording an orange solid. Yield: 0.142 g, 30%. Anal. calcd. for $C_{22}H_{34}Cl_3Ir_2$: C, 33.46; H, 4.31. Found: C, 33.28; H, 4.33. IR (solid): ῡ/cm^{-1} = 2965m, 2905w-m, 2115m, 1995w-m, 1456vs, 1379s, 1158w, 1088w, 1056m, 1030vs, 968m, 825w, 735w-m. ^{1}H NMR (400 MHz, $CDCl_3$): δ/ppm = 2.18 (q, $^3J_{HH}$ = 7.7 Hz, 2 H, CH_2), 1.61, 1.59 (s, 12H, CMe),

1.11 (t, $^{3}J_{HH}$ = 7.7 Hz, 3 H, CH_2CH_3). ^{13}C NMR (400 MHz, $CDCl_3$): δ/ppm = 89.1 (*C*Et), 86.5, 86.2 (*C*Me), 17.6 (CH_2), 11.7 (CH_2CH_3), 9.3, 9.2 (C*Me*). ESI-MS(+) *m/z* = 789.3 $[M–Cl]^+$.

$[^{Pr}Cp^*IrCl(\mu\text{-}Cl)]_2$ (4). The title compound was obtained by using the same procedure described for the synthesis of **3**, from tetramethyl(propyl)cyclopentadiene (0.43 mL, 2.1 mmol) and $IrCl_3 \cdot nH_2O$ (54.6% of Ir, 0.500 g, 1.42 mmol). Orange solid, yield: 0.152 g, 20%. Anal. calcd. for $C_{24}H_{38}Cl_4Ir_2$: C, 33.80; H, 4.46. Found: C, 33.67; H, 4.52. IR (solid): ῡ/cm^{-1} = 2963m-s, 2913m, 2837w, 1450vs, 1381s, 1226w, 1153w, 1086m, 1029vs, 818m-s, 760m, 673m-s.^{1}H NMR (400 MHz, $CDCl_3$): δ/ppm = 2.15, 1.47 (m, 4 H, CH_2), 1.61, 1.59 (s, 12H, CMe), 0.96 (t, $^{3}J_{HH}$ = 7.4 Hz, 3 H, CH_2CH_3). ^{13}C NMR (400 MHz, $CDCl_3$): δ/ppm = 87.9 (*C*Pr), 86.5 (*C*Me), 26.1, 20.9 (CH_2), 14.27 (CH_2CH_3), 9.5, 9.4 (C*Me*). ESI-MS(+) *m/z* = 817.3 $[M–Cl]^+$.

$[^{F\text{-}Ph}Cp^*IrCl(\mu\text{-}Cl)]_2$ (7). The title compound was obtained by using the same procedure described for the synthesis of **3**, from 4-floro-(2,3,4,5-tetramethylcyclopenta-2,4-dien-1-yl)benzene (0.463 g, 2.14 mmol) and $IrCl_3 \cdot nH_2O$ (54.6% of Ir, 0.503 g, 1.43 mmol). The crude product was purified by washing with pentane (2 x 20 mL) and subsequent crystallization from a double layer CH_2Cl_2/pentane at -30 ºC, affording a dark yellow solid. Yield: 0.294 g, 43%. Anal. calcd. for $C_{30}H_{32}Cl_4F_2Ir_2$: C, 37.66; H, 3.35. Found: C, 37.40; H, 3.47. IR (solid): ῡ/cm^{-1} = 3072w, 2992w, 2952w, 2915w, 2774w-m, 2058m, 1985w, 1607m-s, 1518vs, 1458 m-s, 1394w, 1380m-s, 1301w-m, 1227s, 1159s, 1097w-m, 1027m, 994m, 848s, 818s, 743m-w, 721w-m, 676m, 669m. ^{1}H NMR (400 MHz, $CDCl_3$): δ/ppm = 7.57 (dd, $^{4}J_{HF}$ = 5.20 Hz, $^{3}J_{HH}$ = 8.31 Hz, 2 H, C_6H_4), 7.04 (t, $^{3}J_{HF}$ = 8.31 Hz,$^{3}J_{HH}$ = 8.31 Hz, 2 H, C_6H_4), 1.71, 1.60 (s, 12 H, Me). ^{13}CNMR (400 MHz, $CDCl_3$): δ/ppm = 162.9 (d, $^{1}J_{CF}$ = 248 Hz, CF),132.2 (d, $^{3}J_{CF}$ = 8.9 Hz, C_6H_4), 115.9 (d, $^{2}J_{CF}$ = 22.3 Hz, C_6H_4), 125.7 (*C*-C_5Me_4), 93.6, 85.7 (*C*Me), 81.4 (*C*-C_6H_4), 10.3, 9.6 (C*Me*).^{19}F NMR (400 MHz, $CDCl_3$): δ/ppm = –112.7. ESI-MS(+) *m/z* = 921.3 $[M–Cl]^+$. Crystals

of **7** suitable for X-ray analysis were obtained from a concentrated $CDCl_3$ solution stored at -30 °C.

[$^{HO\text{-}Ph}$Cp*IrCl(μ-Cl)]$_2$ (8). A solution of $C_5HMe_4(4\text{-}C_6H_4OCMe_2OMe)$ (0.400 g, 1.40 mmol) and $IrCl_3 \cdot 3H_2O$ (0.350 g, 0.993 mmol) in degassed MeOH (30 mL) was heated at reflux for 72 h under N_2 atmosphere. Afterwards, the reaction mixture was allowed to cool to room temperature, and the volatiles were removed under reduced pressure. The resulting brown oil was charged on a silica column; after elimination of undesired substances with hexane/Et_2O mixtures, an orange fraction was collected by using a mixture of diethyl ether and acetone (1:1 *v/v*) as eluent. The product was obtained as an orange solid upon removal of the volatile materials under vacuum. Yield:0.142 g, 30%. Anal. calcd. for $C_{30}H_{34}Cl_4Ir_2O_2$: C, 37.82; H, 3.60. Found: C, 37.56; H, 3.51. IR (solid): $\tilde{\upsilon}/cm^{-1}$ = 3305m (ν_{OH}), 2921w, 1611m, 1590w, 1519s, 1499w, 1446m, 1376w, 1365w, 1346w, 1265s, 1211m-s, 1173s, 1103w-m, 1031m, 994w, 850vs, 818s, 761m-s, 692m. ^{1}H NMR (400 MHz, CD_3OD): δ/ppm = 7.45 (d, 2 H, $^3J_{HH}$ = 8.3 Hz, C_6H_4), 6.81 (d, 2 H, $^3J_{HH}$ = 8.8 Hz, C_6H_4), 1.68, 1.61 (s, 12 H, C*Me*). ^{13}C NMR (400 MHz, CD_3OD): δ = 157.9 (COH), 131.3, 115.0 (C_6H_4), 120.0 (*C*-C_5Me_4), 93.2, 85.2 (*C*Me), 78.1 (*C*-C_6H_4), 9.1, 8.2 (C*Me*). ESI-MS(+) *m/z* = 952.8 $[M–Cl]^+$.

[^{H}Cp*Ir(κ^2-N,O)Cl] (10, κ^2-N,O = 2-pyridinecarboxylate). Compound **1** (0.128 g, 0.166 mmol), 2-pyridinecarboxylic acid (0.048 g, 0.38 mmol) and sodium methoxide (0.021 g, 0.38mmol) were dissolved in MeOH (20 mL) in the order given. The mixture was refluxed for 3 hours. Afterwards, the solvent was removed, and the crude product was extracted with CH_2Cl_2/H_2O. The organic phase was dried over Na_2SO_4, filtered and concentrated under reduced pressure affording **10** as a yellow solid. Yield: 0.062 g, 40%. Anal. calcd. for $C_{15}H_{17}IrNO_2$: C, 41.37; H, 3.93. Found: C, 41.44; H, 4.00. IR (solid): $\tilde{\upsilon}/cm^{-1}$ = 1651vs, 1602m-s, 1568w, 1494w-

m, 1469w-m, 1441m, 1385w, 1338s, 1304w-m, 1285m, 1264m, 1247m, 1166w-m, 1097m, 1053m, 1029m-s, 849m, 835m, 806m, 787s, 735w-m, 709m, 693m-s, 655 m. ^{1}H NMR (400 MHz, dmso-d_6): δ/ppm = 8.98, 8.16, 7.93, 7.78 (m, 4 H, C_5H_4N), 5.57 (s, 1 H, C_5Me_4*H*), 1.73, 1.67, 1.64, 1.63 (s, 12 H, Me). ^{13}C NMR (400 MHz, dmso-d_6): δ/ppm = 172.8 (OCO), 152.3, 150.6, 140.4, 129.7, 126.9 (C_5H_4N), 92.8, 91.0, 86.7, 83.5 (*C*Me), 67.1 (CH), 10.6, 10.3, 8.9, 8.8 (C*Me*). ESI-MS(+) *m/z* = 436.0 $[M–Cl]^+$.

[^{Pr}Cp*Ir(κ^2-N,O)Cl] (11, κ^2-N,O = 2-pyridinecarboxylate). The title compound was prepared by the same procedure described for the synthesis of **10**, from **4** (0.111 g, 0.130 mmol), 2-pyridinecarboxylic acid (0.039 g, 0.32 mmol) and sodium methoxide (0.017 g, 0.32 mmol). Yellow solid, yield: 0.101 g, 76%. Anal. calcd. for $C_{18}H_{23}ClIrNO_2$: C, 42.14; H, 4.52. Found: C, 42.02; H, 4.58. IR (solid): ῡ/cm^{-1} = 2876w, 1661v-s, 1605m, 1568w, 1495w, 1469m-w, 1456m-w, 1384m-w, 1338s, 1286m, 1244m-w, 1170m, 1112w, 1096m-w, 1056m-w, 1035m, 991w, 960w, 917w, 917m-w, 847m, 827m, 816m-w, 775s, 733w, 706m, 692m, 674 m-w, 658w cm^{-1}. ^{1}H NMR (400 MHz, $CDCl_3$): δ/ppm = 8.57, 8.17, 7.95, 7.57 (m, 4 H, C_5H_4N),2.12 (td, 2 H, J_{HH}= 7.5 and 4.2 Hz, CH_2),1.72, 1.71 (s, 12 H, C*Me*), 1.51 (dq, 2 H, J_{HH}= 15.1 and 7.5 Hz, CH_2),0.97(t, 3 H, $^{3}J_{HH}$ = 7.5 Hz, CH_2CH_3). ^{13}C NMR (400 MHz, $CDCl_3$): δ/ppm = 172.9 (OCO), 151.1, 149.5, 139.3, 128.8, 127.6(C_5H_4N), 86.9, 86.5, 86.0, 85.6 (*C*Me), 25.9, 21.5 (CH_2), 14.2 (CH_2CH_3),9.1, 9.0 (C*Me*). ESI-MS(+) *m/z* = 478.0 $[M–Cl]^+$. Crystals suitable for X-ray analysis were obtained from a dichloromethane solution layered with hexane and stored at -30 °C for one week.

X-ray crystallography. Crystal data and collection details for **7** and **11** are reported in Table 1. Data were recorded on a Bruker APEX II diffractometer equipped with a PHOTON2 detector

using Mo–Kα radiation. Data were corrected for Lorentz polarization and absorption effects (empirical absorption correction SADABS).The structures were solved by direct methods and refined by full-matrix least-squares based on all data using F^2.[53] The crystals of **7** appeared to be non merohedrally twinned. The TwinRotMat routine of PLATON was used to determine the twinning matrix and to write the reflection data file (.hkl) containing the two twin components. Refinement was performed using the instruction HKLF 5 in SHELXL and one BASF parameter, which refined as 0.603(16). The crystals of **11** are racemically twinned with refined Flack parameter 0.394(7).[54] Hydrogen atoms were fixed at calculated positions and refined by a riding model. All non-hydrogen atoms were refined with anisotropic displacement parameters.

WO catalysis driven by $NaIO_4$. Catalytic tests were performed in water at pH 7 by 0.2 M phosphate buffer at 25°C using $NaIO_4$ as a sacrificial oxidant. The formation of molecular oxygen, in the gas phase, was detected with a differential manometer Testo 521-1. Manometric measurements were performed using two homemade-jacketed glass reactors coupled to the manometer. In a typical run, $NaIO_4$, weighed with an analytical balance, was transferred directly into the measuring reactor and dissolved in buffered solution (4.6 – 4.9 mL). The same amount of water was added to the reference reactor. Both reactors were equipped with a side arm to connect to the manometer and a septum to seal the system, which was kept at a constant temperature (T = 25°C). After ca. 20 min, equilibration was reached and the measurement was started. Afterward, 100 – 400 µL of water and catalyst solution were injected into the reference and measuring reactors, respectively. The concentration of the stock solution of catalyst was adjusted, depending on the desired final concentration of the catalyst, to have a final volume of 5 mL. For each complex, the orders in iridium and $NaIO_4$ were determined by varying the catalyst

concentration (1, 2.5, 5, and 10 μM) at [$NaIO_4$] = 20 mM and the $NaIO_4$ concentration (5, 10, 20, 40 mM) at [Ir] = 5 μM, respectively. The multiple addition tests were carried out by adding to the 5 mL of reaction solution 250 μL of $NaIO_4$ solution 0.4 M. Some kinetic measurements were done in duplicate and triplicate to evaluate the error in TOF and TON values, which was found to be approximately equal to 10%. All solvents and reagents were purchased from Sigma – Aldrich and used without any further purification. Purelab Option-R7 (Elga labwater) was used to purify water [resistivity = 18 $M\Omega cm^{-1}$; TOC (total organic carbon) < 20 ppb]. Solutions of $NaIO_4$ for kinetic experiments were prepared by dissolving $NaIO_4$ (ACS reagent, ≥ 99.8%) in ultrapure water. Buffer solutions were prepared by mixing different volumes of previously prepared acid and base stock solutions (0.2 M). pH was checked using a Hanna Instrument pH-meter HI 2221.

Table 1. Crystal data and measurement details for **7** and **11**.

	7	**11**
Formula	$C_{18}H_{23}ClIrNO_2$	$C_{30}H_{32}Cl_4F_2Ir_2$
FW	513.02	956.75
T, K	100(2)	100(2)
λ, Å	0.71073	0.71073
Crystal system	Orthorhombic	Triclinic
Space group	$P2_12_12_1$	$P\bar{1}2$
a, Å	8.2268(3)	8.7487(10)
b, Å	14.3426(6)	17.713(2)
c, Å	14.5746(6)	20.308(3)
α,°	90	73.261(4)
β,°	90	89.913(4)
γ,°	90	83.794(4)
Cell Volume, Å^3	1740.95(12)	2994.6(6)
Z	4	4
D_c, g·cm^{-3}	1.957	2.122
μ, mm^{-1}	7.831	9.267
F(000)	922	1808
Crystal size, mm	0.21×0.18×0.14	0.25×0.18×0.11
θ limits,°	1.980-26.998	1.814-24.999
Reflections collected	25212	40544
Independent reflections	3816 [R_{int} = 0.0371]	10506 [R_{int} = 0.0808]
Data / restraints /parameters	3816 / 0 / 214	10506 /451 / 694
Goodness on fit on F^2	1.189	1.074
R_1 ($I > 2\sigma(I)$)	0.0145	0.0612
wR_2 (all data)	0.0330	0.1479
Absolute structure parameter	0.394(7)	-
Largest diff. peak and hole, e Å^{-3}	0.615 / -0.892	3.229 / -3.698

ASSOCIATED CONTENT

Supporting Information. Complete data and graphics of WO catalytic experiments (Figures S1-S22 and Tables S1-S5); NMR spectra of new compounds (Figures S23-S40). CCDC reference numbers 2014602 (**7**) and 1953420 (**11**) contain the supplementary crystallographic data for the

X-ray studies reported in this paper. These data can be obtained free of charge at www.ccdc.cam.ac.uk/conts/retrieving.html (or from the Cambridge Crystallographic Data Centre, 12, Union Road, Cambridge CB2 1EZ, UK; fax: (internat.) +44-1223/336-033; e-mail: deposit@ccdc.cam.ac.uk).

AUTHOR INFORMATION

Corresponding Author

*Alceo Macchioni - alceo.macchioni@unipg.it

*Fabio Marchetti – Webpage: https://people.unipi.it/fabio_marchetti1974/, Email: fabio.marchetti1974@unipi.it.

Author Contributions

The manuscript was written through contributions of all authors. All authors have given approval to the final version of the manuscript. ⊥ These authors contributed equally.)

ACKNOWLEDGMENT

The University of Perugia and MIUR (AMIS, “Dipartimenti di Eccellenza – 2018 - 2022” programs), the University of Pisa (Fondi di Ateneo 2020), EC (FP7-PEOPLE-2013-CIG, no. 631396), and MINECO (RYC-2012-11231, CTQ2014-60100-R and CTQ2017-84932-P) are gratefully acknowledged for financial support.

REFERENCES

(1) Alstrum-Acevedo, J. H.; Brennaman, M. K.; Meyer, T. J. Chemical Approaches to Artificial Photosynthesis. 2. *Inorg. Chem.* **2005**, *44* (20), 6802–6827 DOI: 10.1021/ic050904r.

(2) Lewis, N. S.; Nocera, D. G. Powering the planet: Chemical challenges in solar energy utilization. *Proc. Natl. Acad. Sci.* **2006**, *103* (43), 15729 LP – 15735 DOI: 10.1073/pnas.0603395103.

(3) Balzani, V.; Credi, A.; Venturi, M. Photochemical conversion of solar energy. *ChemSusChem* **2008**, *1* (1–2), 26–58 DOI: 10.1002/cssc.200700087.

(4) Gust, D.; Moore, T. A.; Moore, A. L. Solar Fuels via Artificial Photosynthesis. *Acc. Chem. Res.* **2009**, *42* (12), 1890–1898 DOI: 10.1021/ar900209b.

(5) McDaniel, N. D.; Bernhard, S. Solar fuels: thermodynamics, candidates, tactics, and figures of merit. *Dalt. Trans.* **2010**, *39* (42), 10021–10030 DOI: 10.1039/C0DT00454E.

(6) Berardi, S.; Drouet, S.; Francàs, L.; Gimbert-Suriñach, C.; Guttentag, M.; Richmond, C.; Stoll, T.; Llobet, A. Molecular artificial photosynthesis. *Chem. Soc. Rev.* **2014**, *43* (22), 7501–7519 DOI: 10.1039/C3CS60405E.

(7) Kanan, M. W.; Nocera, D. G. In Situ Formation of an Water Containing Phosphate and Co 2 +. *Science (80-.).* **2008**, *321* (August), 1072–1075 DOI: 10.1126/science.1162018.

(8) Wang, C.; Wang, J.-L. L.; Lin, W. Elucidating Molecular Iridium Water Oxidation Catalysts Using Metal-Organic Frameworks: A Comprehensive Structural, Catalytic, Spectroscopic, and Kinetic Study. *J. Am. Chem. Soc.* **2012**, *134* (48), 19895–19908 DOI:

10.1021/ja310074j.

(9) McCrory, C. C. L.; Jung, S. H.; Peters, J. C.; Jaramillo, T. F. Benchmarking Heterogeneous Electrocatalysts for the Oxygen Evolution Reaction. *J. Am. Chem. Soc.* **2013**, *135* (45), 16977–16987 DOI: 10.1021/ja407115p.

(10) Fagiolari, L.; Zaccaria, F.; Costantino, F.; Vivani, R.; Mavrokefalos, C. K.; Patzke, G. R.; Macchioni, A. Ir- And Ru-doped layered double hydroxides as affordable heterogeneous catalysts for electrochemical water oxidation. *Dalt. Trans.* **2020**, *49* (8), 2468–2476 DOI: 10.1039/c9dt04306c.

(11) Fagiolari, L.; Bini, M.; Costantino, F.; Gatto, G.; Kropf, A. J.; Marmottini, F.; Nocchetti, M.; Wegener, E. C.; Zaccaria, F.; Delferro, M.; et al. Iridium-Doped Nanosized Zn-Al Layered Double Hydroxides as Efficient Water Oxidation Catalysts. *ACS Appl. Mater. Interfaces* **2020**, *12* (29), 32736–32745 DOI: 10.1021/acsami.0c07925.

(12) Chen, Z.; Concepcion, J. J.; Hu, X.; Yang, W.; Hoertz, P. G.; Meyer, T. J. Concerted O atom-proton transfer in the O-O bond forming step in water oxidation. *Proc. Natl. Acad. Sci. U. S. A.* **2010**, *107* (16), 7225–7229 DOI: 10.1073/pnas.1001132107.

(13) Savini, A.; Bucci, A.; Nocchetti, M.; Vivani, R.; Idriss, H.; Macchioni, A. Activity and Recyclability of an Iridium − EDTA Water Oxidation Catalyst Immobilized onto Rutile TiO 2. *ACS Catal.* **2015**, *5*, 264–271.

(14) Pastori, G.; Wahab, K.; Bucci, A.; Bellachioma, G.; Zuccaccia, C.; Llorca, J.; Idriss, H.; Macchioni, A. Heterogenized Water Oxidation Catalysts Prepared by Immobilizing Kläui-Type Organometallic Precursors. *Chem. - A Eur. J.* **2016**, *22* (38), 13459–13463 DOI:

10.1002/chem.201602008.

(15) Materna, K. L.; Rudshteyn, B.; Brennan, B. J.; Kane, M. H.; Bloomfield, A. J.; Huang, D. L.; Shopov, D. Y.; Batista, V. S.; Crabtree, R. H.; Brudvig, G. W. Heterogenized Iridium Water-Oxidation Catalyst from a Silatrane Precursor. *ACS Catal.* **2016**, *6* (8), 5371–5377 DOI: 10.1021/acscatal.6b01101.

(16) Materna, K. L.; Crabtree, R. H.; Brudvig, G. W. Anchoring groups for photocatalytic water oxidation on metal oxide surfaces. *Chem. Soc. Rev.* **2017**, *46* (20), 6099–6110 DOI: 10.1039/C7CS00314E.

(17) Wan, X.; Wang, L.; Dong, C.-L.; Menendez Rodriguez, G.; Huang, Y.-C.; Macchioni, A.; Shen, S. Activating Kläui-Type Organometallic Precursors at Metal Oxide Surfaces for Enhanced Solar Water Oxidation. *ACS Energy Lett.* **2018**, *3*, 1613–1619 DOI: 10.1021/acsenergylett.8b00847.

(18) Domestici, C.; Tensi, L.; Zaccaria, F.; Kissimina, N.; Valentini, M.; D'Amato, R.; Costantino, F.; Zuccaccia, C.; Macchioni, A. Molecular and heterogenized dinuclear Ir-Cp* water oxidation catalysts bearing EDTA or EDTMP as bridging and anchoring ligands. *Sci. Bull.* **2020**, *65* (19), 1614–1625 DOI: 10.1016/j.scib.2020.06.015.

(19) Duan, L.; Bozoglian, F.; Mandal, S.; Stewart, B.; Privalov, T.; Llobet, A.; Sun, L. A molecular ruthenium catalyst with water-oxidation activity comparable to that of photosystem II. *Nat. Chem.* **2012**, *4* (5), 418–423 DOI: 10.1038/nchem.1301.

(20) Llobet, A. *Molecular Water Oxidation Catalysis*; Llobet, A., Ed.; Wiley, 2014.

(21) Creus, J.; Matheu, R.; Peñafiel, I.; Moonshiram, D.; Blondeau, P.; Benet-Buchholz, J.; García-Antón, J.; Sala, X.; Godard, C.; Llobet, A. A Million Turnover Molecular Anode for Catalytic Water Oxidation. *Angew. Chemie - Int. Ed.* **2016**, *55* (49), 15382–15386 DOI: 10.1002/anie.201609167.

(22) Gerlach, D. L.; Bhagan, S.; Cruce, A. A.; Burks, D. B.; Nieto, I.; Truong, H. T.; Kelley, S. P.; Herbst-Gervasoni, C. J.; Jernigan, K. L.; Bowman, M. K.; et al. Studies of the pathways open to copper water oxidation catalysts containing proximal hydroxy groups during basic electrocatalysis. *Inorg. Chem.* **2014**, *53* (24), 12689–12698 DOI: 10.1021/ic501018a.

(23) Fillol, J. L.; Codolà, Z.; Garcia-Bosch, I.; Gàmez, L.; Pla, J. J.; Costas, M. Efficient water oxidation catalysts based on readily available iron coordination complexes. *Nat. Chem.* **2011**, *3* (10), 807–813 DOI: 10.1038/nchem.1140.

(24) Silva, P.; Vilela, S. M. F.; Tomé, J. P. C.; Almeida Paz, F. A. Multifunctional metal–organic frameworks: from academia to industrial applications. *Chem. Soc. Rev.* **2015**, *44* (19), 6774–6803 DOI: 10.1039/C5CS00307E.

(25) Van Dijk, B.; Rodriguez, G. M.; Wu, L.; Hofmann, J. P.; MacChioni, A.; Hetterscheid, D. G. H. The Influence of the Ligand in the Iridium Mediated Electrocatalyic Water Oxidation. *ACS Catal.* **2020**, *10* (7), 4398–4410 DOI: 10.1021/acscatal.0c00531.

(26) Savini, A.; Bellachioma, G.; Bolaño, S.; Rocchigiani, L.; Zuccaccia, C.; Zuccaccia, D.; Macchioni, A. Iridium-EDTA as an efficient and readily available catalyst for water oxidation. *ChemSusChem* **2012**, *5* (8), 1415–1419 DOI: 10.1002/cssc.201200067.

(27) Corbucci, I.; Albrecht, A. M. M. Iridium Complexes in Water Oxidation Catalysis. In *Iridium(III) in Optoelectronic and Photonics Applications*; 2017.

(28) Macchioni, A. The Middle-Earth between Homogeneous and Heterogeneous Catalysis in Water Oxidation with Iridium. *Eur. J. Inorg. Chem.* **2019**, *2019* (1), 7–17 DOI: 10.1002/ejic.201800798.

(29) Blakemore, J. D.; Schley, N. D.; Balcells, D.; Hull, J. F.; Olack, G. W.; Incarvito, C. D.; Eisenstein, O.; Brudvig, G. W.; Crabtree, R. H. Half-sandwich iridium complexes for homogeneous water-oxidation catalysis. *J. Am. Chem. Soc.* **2010**, *132* (45), 16017–16029 DOI: 10.1021/ja104775j.

(30) Savini, A.; Belanzoni, P.; Bellachioma, G.; Zuccaccia, C.; Zuccaccia, D.; Macchioni, A. Activity and degradation pathways of pentamethyl-cyclopentadienyl-iridium catalysts for water oxidation. *Green Chem.* **2011**, *13* (12), 3360–3374 DOI: 10.1039/c1gc15899f.

(31) Grotjahn, D. B.; Brown, D. B.; Martin, J. K.; Marelius, D. C.; Abadjian, M. C.; Tran, H. N.; Kalyuzhny, G.; Vecchio, K. S.; Specht, Z. G.; Cortes-Llamas, S. A.; et al. Evolution of iridium-based molecular catalysts during water oxidation with ceric ammonium nitrate. *J. Am. Chem. Soc.* **2011**, *133* (47), 19024–19027 DOI: 10.1021/ja203095k.

(32) Zuccaccia, C.; Bellachioma, G.; Bolaño, S.; Rocchigiani, L.; Savini, A.; Macchioni, A. An NMR study of the oxidative degradation of Cp*Ir catalysts for water oxidation: Evidence for a preliminary attack on the quaternary carbon atom of the -C-CH3 moiety. *Eur. J. Inorg. Chem.* **2012**, *2* (9), 1462–1468 DOI: 10.1002/ejic.201100954.

(33) Zuccaccia, C.; Bellachioma, G.; Bortolini, O.; Bucci, A.; Savini, A.; Macchioni, A.

Transformation of a Cp*-iridium(III) precatalyst for water oxidation when exposed to oxidative stress. *Chem. - A Eur. J.* **2014**, *20* (12), 3446–3456 DOI: 10.1002/chem.201304412.

(34) Menendez Rodriguez, G.; Bucci, A.; Hutchinson, R.; Bellachioma, G.; Zuccaccia, C.; Giovagnoli, S.; Idriss, H.; Macchioni, A. Extremely Active, Tunable, and pH-Responsive Iridium Water Oxidation Catalysts. *ACS Energy Lett.* **2017**, *2* (1), 105–110 DOI: 10.1021/acsenergylett.6b00606.

(35) Hintermair, U.; Sheehan, S. W.; Parent, A. R.; Ess, D. H.; Richens, D. T.; Vaccaro, P. H.; Brudvig, G. W.; Crabtree, R. H. Precursor transformation during molecular oxidation catalysis with organometallic iridium complexes. *J. Am. Chem. Soc.* **2013**, *135* (29), 10837–10851 DOI: 10.1021/ja4048762.

(36) Ingram, A. J.; Wolk, A. B.; Flender, C.; Zhang, J.; Johnson, C. J.; Hintermair, U.; Crabtree, R. H.; Johnson, M. A.; Zare, R. N. Modes of activation of organometallic iridium complexes for catalytic water and C-H oxidation. *Inorg. Chem.* **2014**, *53* (1), 423–433 DOI: 10.1021/ic402390t.

(37) Yang, K. R.; Matula, A. J.; Kwon, G.; Hong, J.; Sheehan, S. W.; Thomsen, J. M.; Brudvig, G. W.; Crabtree, R. H.; Tiede, D. M.; Chen, L. X.; et al. Solution structures of highly active molecular ir water-oxidation catalysts from density functional theory combined with high-energy X-ray scattering and EXAFS spectroscopy. *J. Am. Chem. Soc.* **2016**, *138* (17), 5511–5514 DOI: 10.1021/jacs.6b01750.

(38) Rodriguez, G. M.; Gatto, G.; Zuccaccia, C.; Macchioni, A. Benchmarking Water

Oxidation Catalysts Based on Iridium Complexes: Clues and Doubts on the Nature of Active Species. *ChemSusChem* **2017**, *10* (22), 4503–4509 DOI: doi:10.1002/cssc.201701818.

(39) Morris, D. M.; Mcgeagh, M.; Peña, D. De; Merola, J. S. Extending the range of pentasubstituted cyclopentadienyl compounds : The synthesis of a series of tetramethyl (alkyl or aryl) cyclopentadienes (Cp ⁄ R), their iridium complexes and their catalytic activity for asymmetric transfer hydrogenation. *Polyhedron* **2014**, *84*, 120–135 DOI: 10.1016/j.poly.2014.06.053.

(40) Liu, Z.; Habtemariam, A.; Pizarro, A. M.; Fletcher, S. A.; Kisova, A.; Vrana, O.; Salassa, L.; Bruijnincx, P. C. A.; Clarkson, G. J.; Brabec, V.; et al. Organometallic Half-Sandwich Iridium Anticancer Complexes. **2011**, 3011–3026 DOI: 10.1021/jm2000932.

(41) Gibson, C. P.; Bem, D. S.; Falloon, S. B.; Hitchens, T. K.; Cortopassl, J. E.; Virginia, W. Construction of Several Functionally-Substituted Tetramethylcyclopentadienyl Ligands , Their Use in the Syntheses of Several Organometallic Compounds , and Incorporation of the Organometallic Compounds into Polymers. **1992**, No. 5, 1742–1749 DOI: 10.1021/om00040a052.

(42) Gorol, M.; Roesky, H. W.; Noltemeyer, M.; Schmidt, H.; Cyclopentadienyl, K.; P, O. (η 5 -Pentamethylcyclopentadienyl) iridium (III) Complexes with η 2 -N , O and η 2 -P , S Ligands. **2005**, *200500528*, 4840–4844 DOI: 10.1002/ejic.200500528.

(43) Bucci, A.; Savini, A.; Rocchigiani, L.; Zuccaccia, C.; Rizzato, S.; Albinati, A.; Llobet, A.; Macchioni, A. Organometallic iridium catalysts based on pyridinecarboxylate ligands for

the oxidative splitting of water. *Organometallics* **2012**, *31* (23), 8071–8074 DOI: 10.1021/om301024s.

(44) Hao, H.; Liu, X.; Ge, X.; Zhao, Y.; Tian, X.; Ren, T.; Wang, Y. Half-sandwich iridium (III) complexes with α -picolinic acid frameworks and antitumor applications. *J. Inorg. Biochem.* **2019**, *192* (October 2018), 52–61 DOI: 10.1016/j.jinorgbio.2018.12.012.

(45) Blackmond, D. G. Reaction progress kinetic analysis: A powerful methodology for mechanistic studies of complex catalytic reactions. *Angew. Chemie - Int. Ed.* **2005**, *44* (28), 4302–4320 DOI: 10.1002/anie.200462544.

(46) Blackmond, D. G. Kinetic Profiling of Catalytic Organic Reactions as a Mechanistic Tool. *J. Am. Chem. Soc.* **2015**, *137* (34), 10852–10866 DOI: 10.1021/jacs.5b05841.

(47) Mills, A.; Mcmurray, N. Redox Catalysis. *J. Chem. Soc., Faraday Trans. 1* **1989**, *85* (8), 2047–2054.

(48) Mills, A.; Mcmurray, N. Kinetic Study of the Oxidation of Water by CeIV Ions Mediated by Activated Ruthenium Dioxide Hydrate. *J. Chem. Soc., Faraday Trans. 1* **1989**, *85* (8), 2055–2070.

(49) White, C.; Yates, A.; Maitlis, P. M.; Henekey, D. M. (η5-Pentamethylcyclopentadienyl)Rhodium and -Iridium Compounds. *Inorg. Synth.* **1992**, *29*, 228–234.

(50) Menges, F. Spectragryph - optical spectroscopy software, http://www.effemm2.de/spectragryph.

(51) Fulmer, G. R.; Miller, A. J. M.; Sherden, N. H.; Gottlieb, H. E.; Nudelman, A.; Stoltz, B. M.; Bercaw, J. E.; Goldberg, K. I.; Gan, R.; Apiezon, H. NMR Chemical Shifts of Trace Impurities : Common Laboratory Solvents , Organics , and Gases in Deuterated Solvents Relevant to the Organometallic Chemist. *Organometallics* **2010**, *29*, 2176–2179 DOI: 10.1021/om100106e.

(52) Willker, W.; Leibfritz, D.; Kerssebaum, R.; Bermel, W. Gradient Selection in Inverse Heteronuclear Correlation Spectroscopy. *Magn. Reson. Chem.* **1993**, *31*, 287–292.

(53) Sheldrick, G. M. Crystal structure refinement with SHELXL. *Acta Cryst.* **2015**, *C71*, 3–8 DOI: 10.1107/S2053229614024218.

(54) Gendve, U. De. On Enantiomorph-Polarity Estimation. *Acta Cryst.* **1983**, *A39*, 876–881.

BRIEFS (Word Style “BH_Briefs”). If you are submitting your paper to a journal that requires a brief, provide a one-sentence synopsis for inclusion in the Table of Contents.

SYNOPSIS (Word Style “SN_Synopsis_TOC”). If you are submitting your paper to a journal that requires a synopsis, see the journal’s Instructions for Authors for details.